Angular Motion of a Spinning Projectile with a Viscous Liquid Payload

C.H. Murphy*
U.S. Army Armament Research and Development Command, Aberdeen Proving Ground, Maryland

Liquid-payload motion can have a significant effect on the stability of a spinning projectile. A general definition of the pitch and yaw moment exerted by the liquid is developed and expressions are obtained for the frequencies and damping rates of the projectile's angular motion. An expression for the liquid pressure moment is derived without the unnecessary mathematical approximations of the Stewartson-Wedemeyer (SW) theory, and wall shear effects are added to this improved SW pressure moment to obtain the total liquid moment. This moment expression agrees well with experimental results for a Reynolds number as low as 2400 and qualitatively predicts an observed instability for very low Reynolds numbers.

Nomenclature

a = radius of cylinder

a_k = solution of the system, $\sum_k b_{mk} a_k = b_m$

b = radius of the cylindrical air core

$b_k = \int_{-1}^{1} \hat{x} \bar{X}_k(\hat{x})\, d\hat{x}$

$b_{mk} = \int_{-1}^{1} \bar{X}_m(\hat{x}) X_k(\hat{x})\, d\hat{x}$

$C_{\mathrm{LIM}_j}, C_{\mathrm{LIM}}$ = liquid in-plane moment coefficient

C_{LM_j} = fast ($j=1$) or slow ($j=2$) mode liquid moment coefficient defined by Eq. (3)

$C_{\mathrm{LSM}_j}, C_{\mathrm{LSM}}$ = liquid side moment coefficient

C_p = pressure coefficient

$C_{pk}(r)$ = $R_k(r) + (s-2i)s(r/a)a_k$

c = one-half the length of the cylinder

f = $1-(b/a)^2$, the fill ratio

f_j = $1 + (m_L a^2/I_x) C_{\mathrm{LIM}_j}$

I_x, I_y = axial and transverse moments of inertia of the projectile

$J_n(\ )$ = Bessel function of the first kind of order n

$\hat{K}$ = $K_{j0}\exp(i\phi_{j0})$, $j=1$ or 2

K_j = magnitude of the jth yaw arm

K_{j0} = initial value of K_j

k = longitudinal wave number

m_L = $2\pi a^2 c \rho_L$, the liquid mass in a fully filled cylindrical cavity

p = liquid pressure

p_s = liquid pressure perturbation

p_{si} = inviscid part of p_s

p_{sv} = viscous part of p_s

$R\{\ \}$ = real part of $\{\ \}$

Re = $a^2|\dot{\phi}|/\nu$, Reynolds number

r = radial coordinate in an earth-fixed cylindrical system

s = $(\gamma\epsilon + i)\tau$

s_g = gyroscopic stability factor

t = time

u_s, v_s, w_s = components of the liquid velocity perturbation in the earth-fixed cylindrical system x, r, θ

u_{si}, v_{si}, w_{si} = inviscid part of u_s, v_s, w_s

u_{sv}, v_{sv}, w_{sv} = viscous part of u_s, v_s, w_s

V_x, V_r, V_θ = velocity components in the earth-fixed cylindrical system

XYZ = missile-fixed axes, origin at the projectile's center of mass

$X\bar{Y}\bar{Z}$ = aeroballistic nonrolling axes, origin at the projectile's center of mass, Z axis initially downward

$\hat{x}$ = x/c

$Y_n(\ )$ = Bessel function of the second kind of order n

α = $(c/a)[(3+is)/(1+is)]^{1/2}\delta_a^{-1}$

$\tilde{\alpha}$ = angle of attack in the $X\bar{Z}$ plane

β = $i(c/a)[(1-is)/(1+is)]^{1/2}\delta_a^{-1}$

$\tilde{\beta}$ = angle of sideslip in the $X\bar{Y}$ plane

γ = $\dot{\phi}/|\dot{\phi}|$

δ_a = $(1+i)[2(1+is)Re]^{-1/2}$

$\delta_c = \dfrac{-(a/c)\delta_a}{2\sqrt{1+is}}\left[\dfrac{1-is}{\sqrt{3+is}} + i\left(\dfrac{3+is}{\sqrt{1-is}}\right)\right]$

ϵ_j, ϵ = growth rates per cycle

ϵ_{aj} = growth rates per cycle due to aerodynamic moment

θ = azimuthal coordinate in an earth-fixed cylindrical system

λ = $(\pi/2)(1+\delta_c)$

$\hat{\lambda} = \left[\dfrac{s^2-2is+3}{-(s-i)^2}\right]^{1/2}\lambda$

ν = kinematic viscosity

ρ_L = liquid density

σ = I_x/I_y

τ_j, τ = $\dot{\phi}_j/\dot{\phi}$, the nondimensionalized frequency

ϕ = $\dot{\phi}t$

ϕ_j = $\phi_{j0} + \tau_j \dot{\phi} t$ ($j=1,2$)

ϕ_{j0} = initial orientation angle of the jth yaw arm ($j=1,2$)

$\dot{\phi}$ = spin rate

Superscripts

$\bar{(\ )}$ = complex conjugate

$\dot{(\ )}$ = time derivative

$(\ )'$ = derivative with respect to the independent variable involved

Introduction

THE U.S. Army has had a continuing interest in the design of spinning projectiles with liquid payloads. Many of

Received Sept. 27, 1982; revision received Jan. 13, 1983.

*Chief, Launch and Flight Division, Ballistic Research Laboratory. Fellow AIAA.

these developmental shells have shown dramatic instabilities in their pitching and yawing motion. Initially, these instabilities have been identified by large range losses incurred during firing trials. In 1962 Karpov made direct angular motion measurements of liquid-payload-induced instabilities in a 20 mm projectile.[1] In 1973 Mark and Mermagen[2] used solar sensors and telemetry units to observe liquid-payload-induced instabilities in a 155 mm shell. Since that time all developmental shells with liquid payloads have been tested with sunsonde instrumentation and a variety of strange behaviors has been observed.

In 1959 Stewartson published a theoretical paper on the stability of a spinning liquid-filled top.[3] This paper assumed a right circular container partially or fully filled with an *inviscid* fluid. The liquid was assumed to be fully spun-up and in steady-state motion. This motion was assumed to be a circular or spiral motion at a frequency set by the top's static moment and spin rate. The Stewartson theory predicted liquid eigenfrequencies that were to be avoided in order to have stable angular motion of the top. According to the theory, liquid moments would become infinite for coning motion at any of the eigenfrequencies.

In 1965 Karpov[4] made additional 20 mm firings. All shells in this series had the same fast frequencies but the payload eigenfrequencies were varied by use of different cavity fineness ratios. A resonance undamping rate was observed but was of a much smaller amplitude and at a slightly lesser frequency than that predicted by Stewartson.

At about that time Wedemeyer[5] introduced a boundary-layer modification to the Stewartson theory and computed complex liquid eigenvalues. Since the flights at the Ballistic Research Laboratory's (BRL) Aerodynamics Range were too short to allow the liquid to be fully spun-up and in steady-state coning motion, Karpov developed the use of a free liquid-filled gyroscope to measure yaw growth rates near resonance. He found an exceptionally good agreement with the Wedemeyer values at a Reynolds number of 520,000 and fair agreement at a Reynolds number of 5200.[6] Finally, Frasier et al.[7,8] extended this Stewartson-Wedemeyer theory to a cylindrical cavity with a central rod.

The success of Karpov's gyroscope experiments led to extensive use of this technique. This excellent experimental work had the unfortunate effect of biasing most of the later theoretical and experimental work toward understanding liquid-filled gyroscopes and the application to projectiles was treated as a side effect.

A second difficulty with the later gyroscope-oriented work was a tunnel-vision concentration on liquid eigenfrequencies. This was caused by the great success of Wedemeyer's modification of Stewartson's inviscid eigenfrequencies. The basic aim of any liquid-payload theory should be the calculation of the complete moment the liquid payload exerts on the pitching and yawing projectile in flight. Wedemeyer's complex eigenfrequencies identify frequency and damping rate pairs for which the liquid pressure is infinite. For coning motion near any of these pairs, the liquid moment is primarily due to the pressure at the edge of the boundary layer and is dominated by a simple pole function. This pole is an excellent approximation at high Reynolds numbers, but at lower Reynolds numbers it becomes quite poor even though the boundary-layer assumptions are still valid. The pressure at the edge of the boundary layer has to be computed without the pole approximation. In addition, an increment in pressure through the rotating boundary layer on the lateral wall must be computed, as well as the shear on both the lateral and end walls.

It is the aim, then, of this paper to give the general formulation of the effect of liquid-payload motion on projectile stability and to compute the liquid moments, pressures, and wall shears for small-amplitude liquid motion with boundary layers but without the unnecessary mathematical approximations of the Stewartson-Wedemeyer (SW) theory. The results of this new theory will be compared with all available published gyroscope data for Reynolds numbers down to as low as 2400. Finally, the theory will be used at even lower Reynolds numbers to give a theoretical basis for observed instabilities[9,10] caused by very viscous liquids.

Projectile Dynamics

Two coordinate systems, both of which have X axes along the projectile's axis of symmetry, are commonly used: the missile-fixed XYZ system and the aeroballistic $X\tilde{Y}\tilde{Z}$ nonrolling system with the $\tilde{Z}$ axis initially downward. If we introduce earth-fixed axes X_e, Y_e, Z_e with the X_e axis initially along the velocity vector and Z_e downward, a unit vector along the positive X axis has earth-fixed components (n_{XE}, n_{YE}, n_{ZE}). The angle of attack $\tilde{\alpha}$ in the nonrotating system is the angle in the $X\tilde{Z}$ plane from the X axis to the velocity vector, and the angle of sideslip $\tilde{\beta}$ is the angle in the $X\tilde{Y}$ plane from the X axis to the velocity vector.

For small angles the usual dynamics[11] yield a second-order differential equation for $\tilde{\alpha}$ and $\tilde{\beta}$ in terms of a linear aerodynamic force and moment. The solution to this equation is an epicycle which generates the angular motion as the sum of two rotating and damping or undamping two-dimensional vectors

$$\tilde{\beta} + i\tilde{\alpha} = K_1 e^{i\theta_1} + K_2 e^{i\theta_2} \tag{1}$$

where

$$\ell n(K_j/K_{j0}) = \epsilon_j \tau_j |\dot{\phi}| t, \qquad \tau_j = (\sigma/2)\left[1 \pm \sqrt{1-(1/s_g)}\right]$$

Note that for coning motion in the direction of spin, $(\tau_j > 0)$, $\epsilon_j > 0$ for increasing K_j and $\epsilon_j < 0$ for decreasing K_j. For coning motion in the direction opposite to the spin, the inequalities are reversed. Since $\tau_1 > \tau_2$, mode 1 is called the fast mode and mode 2 the slow mode.

Since the liquid moment is the fluid response to the angular motion of the projectile and this motion is the sum of two coning motions [Eq. (1)], the linear liquid moment should be the sum of the responses to each individual coning motion. This condition can be expressed in terms of dimensionless liquid moment coefficients by use of the liquid mass m_L in a fully filled cavity, the spin rate $\dot{\phi}$, and the maximum cavity diameter $2a$,

$$M_{L\tilde{Y}} + iM_{L\tilde{Z}} = m_L a^2 \dot{\phi}^2 \left[\tau_1 C_{\mathrm{LM}_1} K_1 e^{i\phi_1} + \tau_2 C_{\mathrm{LM}_2} K_2 e^{i\phi_2}\right] \tag{2}$$

For linear fluid motion, C_{LM_j} should depend on τ_j, ϵ_j, time, Reynolds number, fill ratio, the shape of the cavity, and the direction of the spin. A similar remark applies to C_{LM_2}. The τ_j appear explicitly in Eq. (2) since the moment should vanish for $\tau_j = 0$. The dependence of these coefficients on time vanishes for the steady-state motion of fully spun-up liquid.

It should be noted that the C_{LM_j} are complex quantities whose imaginary parts represent in-plane moments causing rotations in the plane of $\exp(i\phi_j)$ and whose real parts represent side moments causing rotations out of the plane of $\exp(i\phi_j)$. We therefore introduce the following definition for the real and imaginary parts of C_{LM_j} and explicitly express the effect of the direction of spin,[12]

$$C_{\mathrm{LM}_j} = \gamma C_{\mathrm{LSM}_j} + iC_{\mathrm{LIM}_j} \tag{3}$$

where C_{LSM_j} and C_{LIM_j} are real and represent the liquid side moment and liquid in-plane moment contributions, respectively, and where $\gamma = \dot{\phi}/|\dot{\phi}|$.

A simple interpretation for ϵ_j follows from the observation that for moderate damping, $2\pi\epsilon_j$ is approximately the fractional change in K_j in one cycle. If we restrict this change to be less than 20%, ϵ_j should be less than 0.03.

In general, the liquid moment of Eq. (2) should be combined with the aerodynamic force and moment to give a

somewhat more complicated differential equation for $\tilde{\beta}+i\tilde{\alpha}$. If the epicycle solution [Eq. (1)], is substituted in this new differential equation, new relations for frequency and damping can be obtained,

$$\tau_j = (\sigma/2)\,[f_j - (-1)^j\sqrt{f_j^2 - (1/s_g)}\,] \tag{4}$$

$$\epsilon_j = \epsilon_{aj} + \gamma C_{\mathrm{LSM}_j}\,(m_L a^2/I_x)\,(2\tau_j/\sigma - 1)^{-1} \tag{5}$$

As can be seen from Eq. (5), the liquid side moment has the same effect on the damping of the angular motion as the aerodynamic damping moment. For the fast mode, the coefficient of C_{LSM_1} is positive and a positive side moment causes an undamping of this motion. Similarly a negative C_{LSM_2} will undamp the slow mode. As we shall see, the linear liquid motion theory usually yields a positive side moment, and thus only the fast mode motion is adversely affected by the liquid side moment.

Equations of Liquid Motion

We will consider a projectile with a cylindrical payload cavity with diameter $2a$ and height $2c$. The axis of the cylinder is collinear with the projectile's axis, and its center is located a distance h from the projectile's center of mass. Since h has only a small effect on the liquid moment, we will assume it to be zero for this paper. Exact relations for nonzero h are given in Ref. 12.

If the cavity is partially filled, the liquid is fully spun-up and the centrifugal force is large compared to the aerodynamic forces, then the liquid will fill the space between the outer cylindrical wall and an inner cylindrical free surface with radius b. The ratio of the volume of this inner cylinder to the volume of the complete payload cavity is b^2/a^2. The fill ratio for the payload cavity is, therefore, $1-b^2/a^2$ and will be denoted by f. However, m_L will always be the liquid mass in a fully filled cavity.

The objective of the linear theory is to predict the liquid moment response to coning or spiral motion of the form

$$\tilde{\beta}+i\tilde{\alpha} = K_j e^{i\phi_j} = \hat{K}e^{s\phi}, \qquad j = 1 \text{ or } 2 \tag{6}$$

The components of the velocity of any point on the projectile in earth-fixed cylindrical coordinates are[12]

$$V_x = R\{\dot{\phi}(s-i)r\hat{K}e^{s\phi - i\theta}\} \tag{7}$$

$$V_r = -R\{\dot{\phi}(s-i)x\hat{K}e^{s\phi - i\theta}\} \tag{8}$$

$$V_\theta = r\dot{\phi} + R\{i\dot{\phi}(s-i)x\hat{K}e^{s\phi - i\theta}\} \tag{9}$$

where $R\{\ \} = [\{\ \} + \{\bar{\ }\}]/2$ is the real part of a complex quantity.

We will now make the very restrictive assumption that the liquid is in steady-state response to the coning and spinning motion of the projectile. Theoretical studies[13,14] have been made and are in progress to determine the effect of partially spun-up liquid, and an experimental study of the transient response to coning motion has been made.[15] These studies show that spin-up and cone-up effects are large and important to a complete understanding of the liquid payload stability problem.

Nevertheless, we will assume that the liquid velocity components and liquid pressure have the same dependency on time and θ as the velocity components of points on the projectile and introduce four small dimensionless functions of r and x: u_s, v_s, w_s, and p_s,

$$V_x = R\{u_s e^{s\phi - i\theta}\}(a\dot{\phi}) \tag{10}$$

$$V_r = R\{v_s e^{s\phi - i\theta}\}(a\dot{\phi}) \tag{11}$$

$$V_\theta = r\dot{\phi} + R\{w_s e^{s\phi - i\theta}\}(a\dot{\phi}) \tag{12}$$

$$p = \rho_L(r^2\dot{\phi}^2/2) + R\{p_s e^{s\phi - i\theta}\}(\rho_L a^2\dot{\phi}^2) \tag{13}$$

Equations (10-13) can now be placed in the linearized unsteady Navier-Stokes equations and the continuity equation to yield

$$(s-i)v_s - 2w_s + a\frac{\partial p_s}{\partial r} = \gamma Re^{-1}\left[\nabla_\theta^2 v_s - \frac{a^2 v_s}{r^2} + \frac{2a^2 i w_s}{r^2}\right] \tag{14}$$

$$(s-i)w_s + 2v_s - \frac{iap_s}{r} = \gamma Re^{-1}\left[\nabla_\theta^2 w_s - \frac{a^2 w_s}{r^2} - \frac{2a^2 i v_s}{r^2}\right] \tag{15}$$

$$(s-i)u_s + a\frac{\partial p_s}{\partial x} = \gamma Re^{-1}\nabla_\theta^2 u_s \tag{16}$$

$$\frac{\partial(rv_s)}{\partial r} - iw_s + r\frac{\partial u_s}{\partial x} = 0 \tag{17}$$

where

$$\nabla_\theta^2 = a^2\left[\frac{\partial^2}{\partial r^2} + \frac{\partial}{r\partial r} + \frac{\partial^2}{\partial x^2} - \frac{1}{r^2}\right]$$

Since the effect of negative spin can easily be found from Eq. (3), only positive spin ($\gamma = 1$) will be considered for the remainder of this paper.

Boundary-Layer Solution

Wedemeyer[5] made the assumption that the velocity components and pressure could each be expressed as the sum of inviscid and viscous terms. The inviscid terms satisfy Eqs. (14-17) for $Re^{-1} = 0$ over the entire cylinder except for a small boundary-layer region near the cylinder walls, while the viscous terms satisfy the boundary-layer versions of Eqs. (14-17). Although Wedemeyer considered the effect of these boundary-layer terms only on the liquid eigenvalues, this paper will consider all of their contributions to the liquid moment.

Far from the lateral wall, the viscous terms, u_{sv}, v_{sv}, w_{sv}, and p_{sv}, must vanish. Near the wall, the velocities must be those required by Eqs. (7-9), that is, near $r = a$,

$$u_{sv} = -[(i-s)\hat{K} + u_{si}]e^{(r-a)/a\delta_a} \tag{18}$$

$$w_{sv} = [(1+is)(x/a)\hat{K} - w_{si}]e^{(r-a)/a\delta_a} \tag{19}$$

$$p_{sv} = (2/a)\int w_{sv}\,dr \tag{20}$$

and for $r = a$,

$$v_{si} - a\delta_a\frac{\partial v_{si}}{\partial r} = (i-s)\left(\frac{x}{a}\right)\hat{K} \tag{21}$$

Near the end walls, $\hat{x} \equiv x/c = \pm 1$,

$$w_{sv} + iv_{sv} = -(w_{si} + iv_{si})e^{-\alpha(1 \mp \hat{x})} \tag{22}$$

$$w_{sv} - iv_{sv} = -[w_{si} - iv_{si} \mp 2(1+is)(c/a)\hat{K}]e^{-\beta(1 \mp \hat{x})} \tag{23}$$

$$p_{sv} = 0 \tag{24}$$

and for $\hat{x} = \pm 1$,

$$u_{si} \mp \delta_c\frac{\partial u_{si}}{\partial \hat{x}} = -(i-s)\left(\frac{r}{a}\right)\hat{K} \tag{25}$$

It is interesting to note that according to Eq. (24) the usual boundary condition of no pressure change through the boundary layer is present. Equation (20) shows that this is not the case on the lateral wall. The pressure at the wall differs

from that at the edge of the boundary layer by $p_{sv}(a)$. This pressure difference can be computed by inserting w_{sv} as given by Eq. (19) in Eq. (20) and integrating,

$$p_{sv}(a,\hat{x}) = 2\delta_a [(1+is)(c/a)\hat{x}\hat{K} - w_{si}(a,\hat{x})] \quad (26)$$

Pressure Moment

The major components of the liquid moment are due to the pressure on the lateral and end walls of the container. Lesser components are due to the viscous wall shear on the lateral and end walls. Thus the liquid moment coefficient can be given as a sum of four terms,

$$\tau C_{\mathrm{LM}} = m_{pl} + m_{pe} + m_{vl} + m_{ve} \quad (27)$$

The sum of the first two terms is the pressure moment coefficient m_p and will be computed in this section. The wall shear moment coefficient will be computed in the next section.

The fluctuating part of the inviscid pressure given by Eq. (13) is the sum of the pressure perturbation and a centrifugal term,[12]

$$\frac{\Delta p}{\rho_L a^2 \dot{\phi}^2} = R\left\{\left[p_{si} - \left(\frac{rx}{a^2}\right)\hat{K}\right]e^{s\phi - i\theta}\right\} = R\{C_p e^{i\phi_p}\hat{K}e^{(s\phi - i\theta)}\} \quad (28)$$

The inviscid ($Re = \infty$) version of Eqs. (14-17) can be solved to yield a series for the pressure coefficient,

$$C_p e^{i\phi_p} = -\frac{c}{a}\sum_{k=1}^{N} X_k(\hat{x}) C_{pk}(r) \quad (29)$$

$$X_k = \sin(k\lambda\hat{x}), \qquad k \text{ odd} \quad (30)$$

The pressure moment coefficient on the lateral wall can be computed by an integral of the *real* pressure over this wall, with the appropriate lever arm,

$$m_{pl} = \frac{ice^{-s\phi}}{2\pi a\hat{K}}\int_{-1}^{1}\int_{0}^{2\pi} \hat{x}R\{C_p^* e^{s\phi - i\theta}\}\Big|_{r=a} e^{i\theta}\,d\theta\,d\hat{x}$$

$$= i\left(\frac{c}{2a\hat{K}}\right)\int_{-1}^{1}\hat{x}[C_p^*]_{r=a}\,d\hat{x} \quad (31)$$

where $C_p^* = C_p\hat{K}e^{i\phi_p} + p_{sv}$. Since the complex pressure dependence on $\hat{x}$ is a sum of sine functions, this integral can be easily evaluated.

The end wall pressure moment coefficient is the difference of two similar integrals on each end wall,

$$m_{pe} = -i(2\pi a^2 c\hat{K})^{-1}e^{-s\phi}\int_b^a\int_0^{2\pi} m_{pe}^* e^{\theta\theta}\,d\theta\,dr$$

$$= -i\left(\frac{a}{2c}\right)a^{-3}\int_b^a [C_p e^{i\phi_p}]_{\hat{x}=-1}^{\hat{x}=1} r^2\,dr \quad (32)$$

where

$$m_{pe}^* = r^2 R\{C_p\hat{K}e^{s\phi + i(\phi_p - \theta)}\}_{\hat{x}=-1}^{\hat{x}=1}$$

This moment coefficient involves the integrals of Bessel functions but these particular integrals can be easily obtained in closed form.[16] Equations (29-32) have been coded for $N = 19$ by Bradley.[17]

Stewartson[3] incorrectly used a complex Δp in his pressure integral and, therefore, his moment calculation lacks the half factors of Eqs. (31) and (32). Later he made a similar error of a factor of two in computing a complex direction cosine so that these cancelling errors give the correct yaw growth rates ϵ_j. When modified by Wedemeyer,[5] these yaw growth rates gave outstanding agreement with gyroscope measurements for large Reynolds numbers.

Wall Shear Moment

In addition to the pitch and yaw moment due to pressure on the walls of the liquid container, moments due to viscous wall shear are present. These can be computed from the derivatives of the viscous velocity components of the boundary-layer solution. The liquid moment coefficient due to the shear on the cylindrical lateral wall is

$$m_{vl} = i(2\pi\hat{K}Re)^{-1}e^{-s\phi}\int_{-1}^{1}\int_{0}^{2\pi} e^{i\theta}m_{vl}^*\,d\theta\,d\hat{x} \quad (33)$$

where

$$m_{vl}^* = aR\left\{\frac{\partial u_{sv}}{\partial r}e^{s\phi - i\theta}\right\} - ixR\left\{\frac{\partial w_{sv}}{\partial r}e^{s\phi - i\theta}\right\}$$

Equation (33) simplifies to

$$m_{vl} = (2\hat{K}Re)^{-1}\int_{-1}^{1}\left[ia\frac{\partial u_{sv}}{\partial r} + c\hat{x}\frac{\partial w_{sv}}{\partial r}\right]_{r=a} d\hat{x} \quad (34)$$

The velocity derivatives in Eq. (34) can be computed from Eqs. (18) and (19) and the resulting equation has been coded by Bradley.[17]

The wall shear moment coefficient on the forward flat end wall is

$$m_{ve_l} = (2\pi ac\hat{K}Re)^{-1}e^{-s\phi}\int_b^a\int_0^{2\pi} e^{i\theta}m_{vel}^*\,r\,d\theta\,dr \quad (35)$$

where

$$m_{ve_l}^* = c\left[R\left\{\frac{\partial w_{sv}}{\partial x}e^{s\phi - i\theta}\right\} - iR\left\{\frac{\partial v_{sv}}{\partial x}e^{s\phi - i\theta}\right\}\right]_{\hat{x}=1}$$

A similar expression applies for the rearward end wall. The sum of these moment coefficients has the simple form

$$m_{ve_l}^* = (a\hat{K}Re)^{-1}\int_b^a\left[\frac{\partial}{\partial x}(w_{sv} - iv_{sv})\right]_{\hat{x}=1} r\,dr \quad (36)$$

Discussion

Our theory allows us to calculate C_{LSM} and C_{LIM} as functions of fill ratio f, fineness ratio c/a, Reynolds number Re, dimensionless frequency τ, and yaw growth rate per cycle ϵ. (For the mode 1 coning or spiral motion of Eq. (6), we will drop the j subscript on C_{LSM}, C_{LIM}, τ, and ϵ.) As an example, we will consider a 100% filled cylinder with a fineness ratio of 3.24. Stewartson's inviscid theory predicts a large liquid moment near $\tau = 0.07$.

For a Reynolds number of 500,000, the pressure components of C_{LSM} and C_{LIM} have been computed as functions of τ for τ between 0 and 0.14 and plotted in Figs. 1 and 2. Two values of ϵ are shown in these figures ($\epsilon = 0$ and 0.02) and it can be seen that the moment coefficients are strongly dependent on the yaw growth rate near the eigenfrequency of 0.07 at this Reynolds number.

Figure 3 shows the pressure component of the liquid side moment coefficient for the much lower Reynolds number of 15,000. The effect of the increased viscosity is to decrease the influence of ϵ and to reduce the peak side moment coefficient by a factor of 4.3. The Wedemeyer approximate theory[5] predicts this peak to vary as $Re^{-1/2}$. For this case the predicted factor is 5.8 and thus the Wedemeyer approximation is poor for Re of 15,000, although a complete boundary-layer theory should still be valid.

For a Reynolds number of 500,000, the liquid side moment is dominated by the pressure component. If the pressure at the junction of the cylindrical sidewall and a flat end wall is considered, it is clear that the pitch moment on the lateral wall

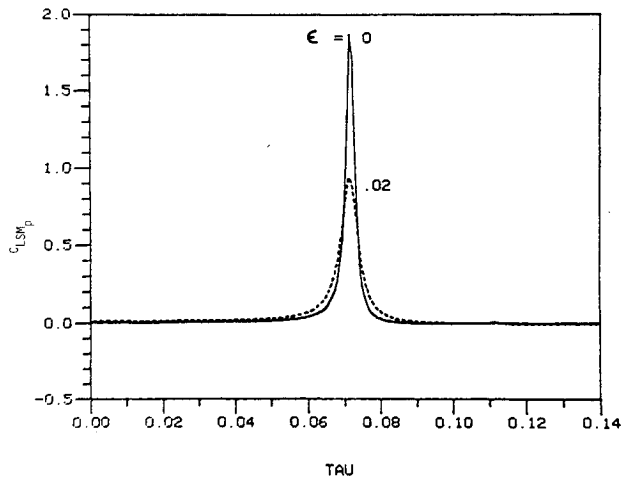

Fig. 1 Pressure component of $C_{LSM}(\tau)$ for $Re = 500{,}000$, $c/a = 3.24$, $f = 1$, $\epsilon = 0, 0.02$.

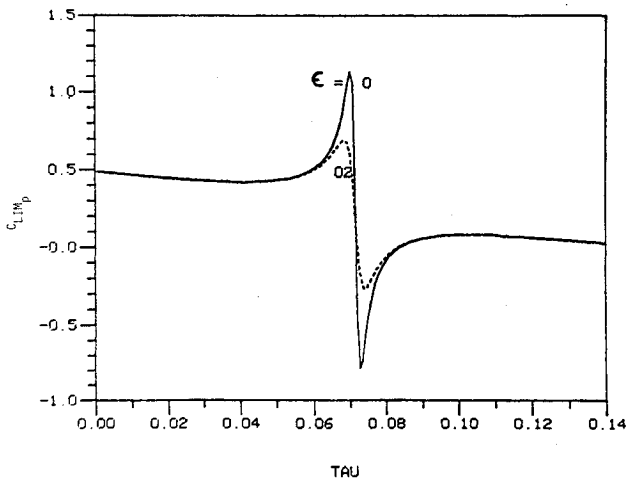

Fig. 2 Pressure component of $C_{LIM}(\tau)$ for $Re = 500{,}000$, $c/a = 3.24$, $f = 1$, $\epsilon = 0, 0.02$.

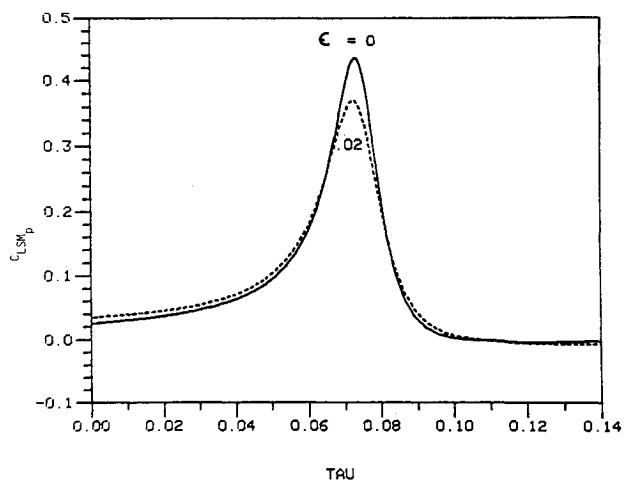

Fig. 3 Pressure component of $C_{LSM}(\tau)$ for $Re = 15{,}000$, $c/a = 3.24$, $f = 1$, $\epsilon = 0, 0.02$.

should oppose that on the end walls. Indeed, at the eigenfrequency, the lateral wall pressure component of the liquid side moment is only 20% larger than the sum of the two end wall pressure components and opposes them. Thus, a small percentage change in the pressure on one of these walls would have a large effect on the total liquid side moment.

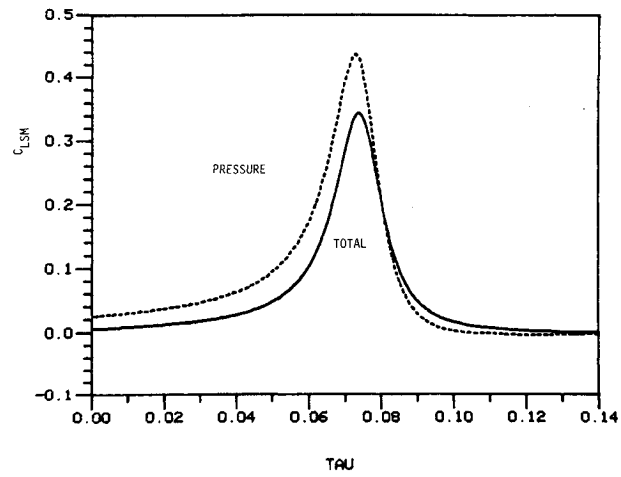

Fig. 4 $C_{LSM}(\tau)$ and its pressure component for $Re = 15{,}000$, $c/a = 3.24$, $f = 1$, $\epsilon = 0$.

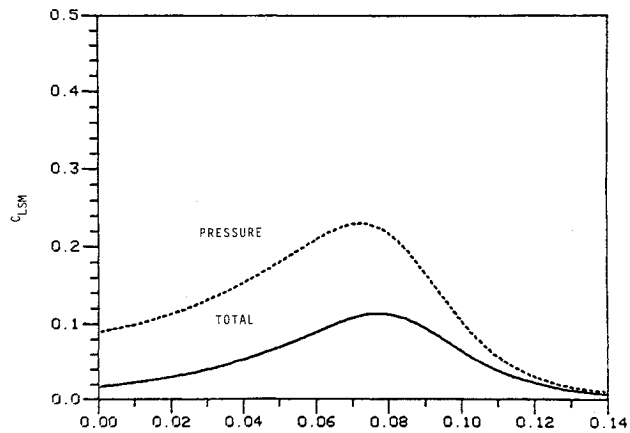

Fig. 5 $C_{LSM}(\tau)$ and its pressure component for $Re = 1{,}000$, $c/a = 3.24$, $f = 1$, $\epsilon = 0$.

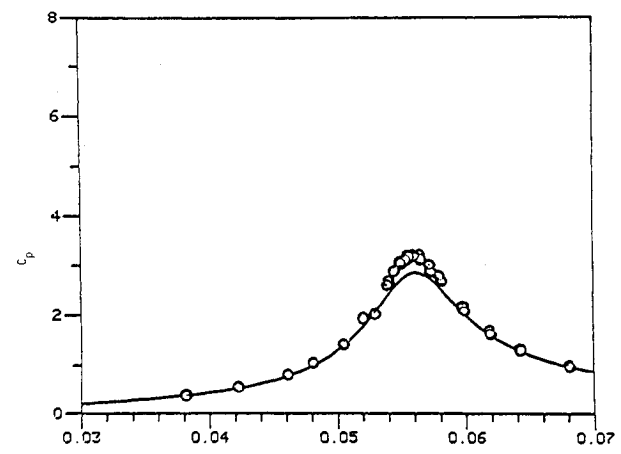

Fig. 6 $C_p(\tau)$ for a partially filled cavity ($f = 0.92$), predicted curve and Whiting data (see Ref. 18, Fig. 10g), $Re = 80{,}000$, $c/a = 3.148$, transducer at $r/a = 0.668$.

At the lower Reynolds number of 15,000, the wall shear component is over a third of the total side moment coefficient and must be considered. In Fig. 4 the pressure component of the liquid side moment coefficient is replotted as a dotted line and compared with the total liquid side moment coefficient, which includes the wall shear terms. Figure 5 makes this comparison at the even lower Re value of 1000 and the wall shear terms are seen to be the same size as the pressure terms and oppositely directed.

Experimental Results

In 1980 the first wall pressure measurements in a precessing and spinning liquid-filled cylinder were made by Whiting.[18] For the 100% filled cylinder, he compared his measurements with theoretical calculations by Gerber et al.[19,20] Gerber's theory was developed for fully filled cylinders only and was used to compute the viscous influence of the lateral wall exactly without the use of a boundary-layer approximation. Its results for fully filled cylinders should, therefore, be better than that of this report when they differ. For the Reynolds numbers of the Whiting tests, they did not differ significantly and, thus, the good experimental agreement Whiting found for Gerber's calculations also applies to our theory. In two cases, however, Whiting measured the pressure on the flat end wall of a partially filled cylinder ($f=0.92$). A comparison of Whiting's measurements for the lower Re of 80,000 with the theoretical prediction of Eq. (29) is given in Fig. 6. The agreement with theory is quite satisfactory.

In most gyroscope experiments[6,21] the yaw growth rates and coning rates are measured for a variety of test conditions. In all experiments the center of mass is located at the pivot point so that the gyroscopic stability factor is infinitely large and Eqs. (4) and (5) for frequency and damping become

$$\tau=\sigma[1+(m_L a^2/I_x)\,C_{\mathrm{LIM}}]\doteq\sigma \tag{37}$$

$$\epsilon=(m_L a^2/I_x)\,(2\tau/\sigma-1)^{-1}C_{\mathrm{LSM}}(\tau,\epsilon) \tag{38}$$

Although good agreement[12] was obtained between the theory and the data analyzed in Ref. 6, the lowest Reynolds number tested was 5200. D'Amico and Rogers[21] made yaw growth rate measurements at Reynolds numbers of 12,400 and 2400 on a 100% filled cylinder with a fineness ratio of 1.042 and, therefore, can provide the best test of the theory. For this case an eigenfrequency exists at 0.040 and the coning frequency was varied from 0.040-0.100 by varying I_y. Comparisons of theory with data are shown in Figs. 7 and 8. Agreement is fair, but there appears to be a systematic bias. Theoretical curves for different fineness ratios in steps of 0.001 were computed and the best fits are shown as dashed curves for $c/a=1.047$ and 1.048 in the respective figures. An effective fineness ratio 0.5% greater than the measured value is not unreasonable and gives excellent experimental agreement.

In Ref. 20, Gerber and Sedney compute liquid side moments from a linearized Navier-Stokes theory and compare it with some unpublished data obtained by D'Amico for $c/a=1.042$ and $Re=5000$ and 1000. As might be expected, for these low Reynolds numbers the linear Navier-Stokes theory gave much better agreement with the data than the linear boundary-layer theory of this paper.

Low Reynolds Number Instability

In a special gyroscope experiment, Miller[9] forced a spinning cylinder filled with liquid to precess at an angle of 20 deg and measured the despin moment. The fineness ratio was 4.29 and liquids with kinematic viscosities ranging between 1 and 10^6 cs were used. A coning rate of 8.3 Hz was forced and the spin was allowed to vary between 67 and 33 Hz. This corresponds to τ varying between 0.12 and 0.25. The measured despin moment varied from a small value for water ($\nu=1$ cs) to a peak value 30 times larger for corn syrup ($\nu=2\times10^5$ cs). The Reynolds number of this peak was about 10.

It was conjectured that this large despin moment would be associated with a large side moment which would produce flight instabilities. Flight tests were made and this otherwise unexpected instability was observed.[10] The theory of this paper can be used to compute the liquid side moment for Miller's cylinder and the largest possible range of Reynolds number. Since 100 is probably the extreme lower bound of Reynolds number for a boundary-layer theory, this range will extend from 1,000,000 to 100.

In Fig. 9, C_{LSM} is plotted vs τ for $Re=10^6$ and four local maxima can be seen. These four eigenfrequencies probably do

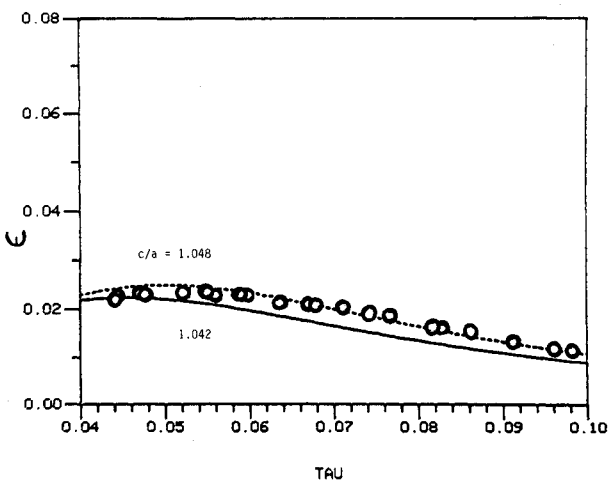

Fig. 8 $\epsilon(\tau)$ for a fully filled cavity, predicted curve and D'Amico data (see Ref. 21, Fig. 6), $Re=2400$, $c/a=1.042$ (nominal) and 1.048 (fitted), $m_L a^2/I_x=0.0632$.

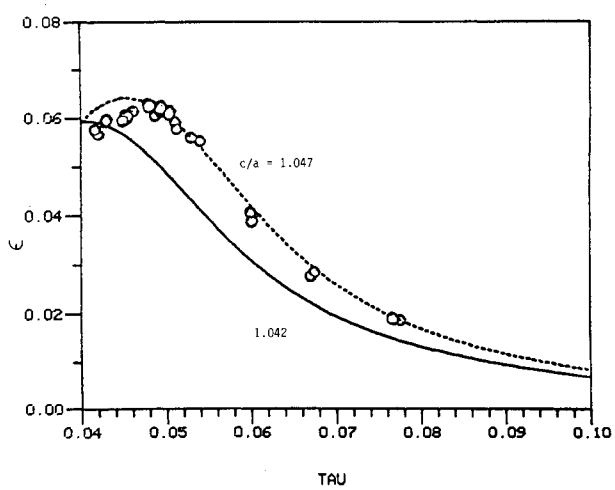

Fig. 7 $\epsilon(\tau)$ for a fully filled cavity, predicted curve and D'Amico data (see Ref. 21, Fig. 5), $Re=12{,}400$, $c/a=1.042$ (nominal) and 1.047 (fitted), $m_L a^2/I_x=0.0833$.

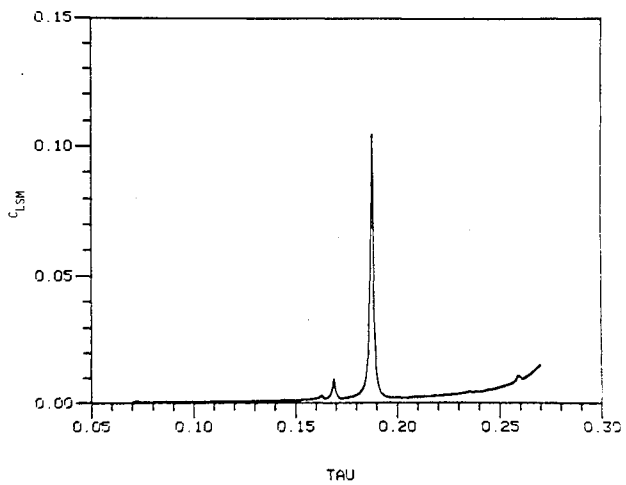

Fig. 9 $C_{LSM}(\tau)$ for $Re=10^6$, $\epsilon=0$, and the D'Amico-Miller parameter values: $c/a=4.291$, $f=1$.

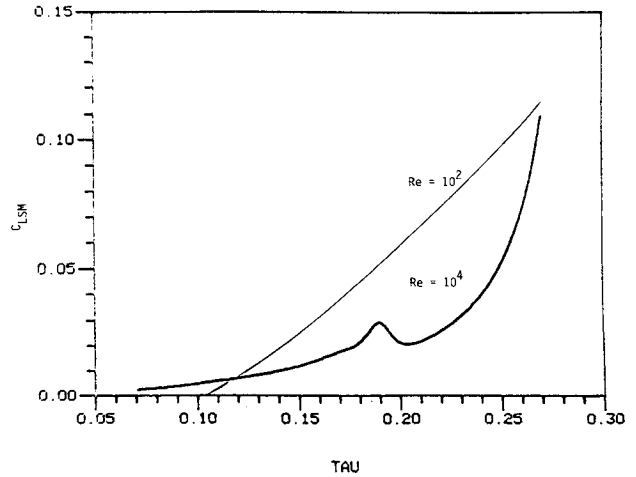

Fig. 10 $C_{LSM}(\tau)$ for $Re = 10^4$ and 10^2, $\epsilon = 0$, and the D'Amico-Miller parameter values: $c/a = 4.291, f = 1$.

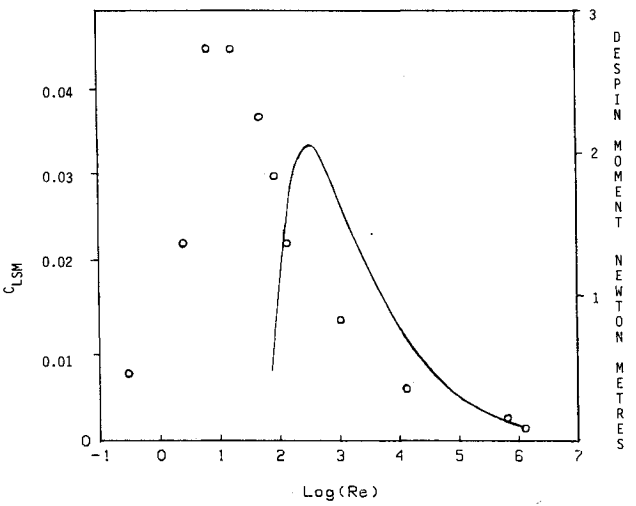

Fig. 11 $C_{LSM}(Re)$ for $\tau = 0.15$, $\epsilon = 0$, $f = 1$, $c/a = 4.291$, $f = 1$, $c/a = 4.291$ [circles are despin moment values, normalized by water density, from the D'Amico-Miller experiment (see Refs. 9 and 10)].

not affect Miller's experiment for water due to his rapidly varying τ. Figure 10 shows the liquid side moment coefficient for Re of 10^4 and 10^2 and Fig. 11 is a cross plot vs logRe of the liquid side moment coefficient for $\tau = 0.15$.

The effect of the increasing viscosity is to smooth out the local maxima and raise the general level of the curve. Indeed, the cross plot shows a maximum at Re of 300. For comparison, Miller's despin moment is superimposed on this plot. The qualitative agreement is impressive.

Summary

1) A general definition of the liquid moment has been developed, and the expression for frequencies and damping of projectile angular motion has been obtained.

2) An exact pressure moment has been computed for the linear boundary theory.

3) Wall shear effects have been added to the exact pressure moment.

4) Good agreement with low Reynolds number experimental data has been shown.

5) The improved theory shows a decrease in the size of eigenfrequency-associated peaks in the side moment with decreasing Reynolds number.

6) The average level of the side moment, however, grows with decreasing Reynolds number to a peak, in good qualitative agreement with the D'Amico-Miller conjecture.

References

[1] Karpov, B.G., "Experimental Observations of the Dynamic Behavior of Liquid-Filled Shell," BRL Rept. 1171, Aug. 1961 (AD 287142).

[2] Mark, A. and Mermagen, W.H., "Measurement of Spin Decay and Instability of Liquid-Filled Projectiles via Telemetry," BRL Memorandum Rept. 2333, Oct. 1973 (AD 771919).

[3] Stewartson, K., "On the Stability of a Spinning Top Containing Liquid," *Journal of Fluid Mechanics,* Vol. 5, Pt. 4, Sept. 1959, pp. 577-592.

[4] Karpov, B.G., "Dynamics of Liquid-Filled Shell: Resonance and Effect of Viscosity," BRL Rept. 1279, May 1965 (AD 468054).

[5] Wedemeyer, E.H., "Viscous Corrections to Stewartson's Stability Criterion," BRL Rept. 1325, June 1966 (AD 489687).

[6] Whiting, R.D. and Gerber, N., "Dynamics of a Liquid-Filled Gyroscope: Update of Theory and Experiment," BRL Tech. Rept. ARBRL-TR-02221, March 1980 (AD A083886).

[7] Frasier, J.T. and Scott, W.E., "Dynamics of a Liquid-Filled Shell: Cylindrical Cavity with a Central Rod," BRL Rept. 1391, Feb. 1968 (AD 667365).

[8] Frasier, J.T., "Dynamics of a Liquid-Filled Shell: Viscous Effects in a Cylindrical Cavity with a Central Rod," BRL Memorandum Rept. 1959, Jan. 1969 (AD 684344).

[9] Miller, M.C., "Flight Instabilities of Spinning Projectiles Having Nonrigid Payloads," *Journal of Guidance, Control, and Dynamics,* Vol. 5, March-April 1982, pp. 151-157.

[10] D'Amico, W.P. and Miller, M.C., "Flight Instability Produced by a Rapidly Spinning, Highly Viscous Liquid," *Journal of Spacecraft and Rockets,* Vol. 16, Jan.-Feb. 1979, pp. 62-64.

[11] Murphy, C.H., "Free Flight Motion of Symmetric Missiles," BRL Rept. 1216, July 1963 (AD 442757).

[12] Murphy, C.H., "Angular Motion of a Spinning Projectile with a Viscous Liquid Payload," BRL Memorandum Rept. ARBRL-MR-03194, Aug. 1982 (AD A118676).

[13] Lynn, Y.M., "Free Oscillations of a Liquid During Spin-Up," BRL Rept. 1663, Aug. 1973 (AD 769710).

[14] Kitchens, C.W., Gerber, N., and Sedney, R., "Oscillations of a Liquid in a Rotating Cylinder, Part I: Solid-Body Rotation," BRL Technical Rept. ARBRL-TR-02081, June 1978 (AD A057759).

[15] D'Amico, W.P., Beims, W.G., and Rogers, T.H., "Pressure Measurements of a Rotating Liquid for Impulsive Coning Motion," BRL Memorandum Rept. ARBRL-MR-03208, Nov. 1982 (AD A121603). (See also AIAA Paper 82-0249, Jan. 1982.)

[16] McLachlan, N.W., *Bessel Functions for Engineers,* Oxford University Press, London, 1955.

[17] Bradley, J.W., "Calculations of Liquid Payload Moment," BRL Memorandum Rept., in preparation.

[18] Whiting, R.D., "An Experimental Study of Forced Asymmetric Oscillations in a Rotating Liquid-Filled Cylinder," BRL Technical Rept. ARBRL-TR-02376, Oct. 1981 (AD A107948).

[19] Gerber, N., Sedney, R., and Bartos, J.M., "Pressure Moment on a Liquid-Filled Projectile: Solid Body Rotation," BRL Technical Rept. ARBRL-TR-02422, Oct. 1982 (AD A120567).

[20] Gerber, N. and Sedney, R., "Moment on a Liquid-Filled Spinning and Nutating Projectile: Solid Body Rotation," BRL Technical Rept., AR BRL-TR-02470, Feb. 1983, AD A125332.

[21] D'Amico, W.P. and Rogers, T.H., "Yaw Instabilities Produced by Rapidly Rotating, Highly Viscous Liquids," AIAA Paper 81-0224, Jan. 1981.